Seeded growth of hydroxyapatite in simulated body fluid

N. SPANOS
School of Science and Technology, Hellenic Open University, Patras, GR 26222, Greece; Institute of Chemical Engineering and High Temperature Chemical Processes, P.O. Box 1414, Patras, GR 26504, Greece

D. Y. MISIRLIS
Department of Chemical Engineering, University of Patras, Patras, GR 26504, Greece

D. G. KANELLOPOULOU, P. G. KOUTSOUKOS*
Institute of Chemical Engineering and High Temperature Chemical Processes, P.O. Box 1414, Patras, GR 26504, Greece; Department of Chemical Engineering, University of Patras, Patras, GR 26504, Greece
E-mail: pgk@iceht.forth.gr

Published online: 17 February 2006

The precipitation of calcium phosphates was investigated, in simulated body fluid (SBF), pH 7.40 and 37°C. The kinetics of the mineral phase forming in the SBF was measured using the constant supersaturation method. The approach provides a detailed investigation in the processes taking place in the SBF which is widely used for the study of biomineralization. The pH adjustment was done by a pH-stat instead of Tris-Buffer [Tris (hydroxymethyl) Aminomethane] to avoid the presence of organic soluble compounds. The stability of SBF was investigated and the stable supersaturated solutions were seeded. The technique of seeded precipitation was employed for the achievement of accurate and reproducible kinetics measurements. The crystal growth experiments in which SBF solutions of variable supersaturations were seeded with hydroxyapatite [$Ca_5(PO_4)_3OH$, HAP] crystals showed that the precipitation of calcium phosphates took place exclusively on specific active sites provided on the surface of the synthetic seed crystals. The crystal growth mechanism showed that the process was controlled by surface diffusion. The phase formed was HAP in the lattice of which CO_3^{2-} and Mg^{2+} ions were incorporated. SBF was the source of these ions. Moreover it was found that the less stable calcium phosphate dihydrate ($CaHPO_4{\cdot}2H_2O$, DCPD) may form as a transient phase hydrolyzing rapidly into the more stable HAP. Morphological examination of the carbonated apatites formed in the SBF showed appreciable aggregation.

1. Introduction

Calcification or deposition of calcium salts, is an important process for the formation of bone and teeth in higher mammals. Pathological calcification on the contrary is the cause of failure of vital organs. The inorganic component of the calcified deposits consists mainly of calcium phosphates. Biological fluids are supersaturated with respect to these salts resulting in their deposition in the hard tissues, on the vascular walls and generally on the surfaces which are in contact with blood serum, such as implants, heart valves etc. The calcium phosphate system is complicated as it involves a number of salts of variable stability, in the order of decreasing solubility: Dicalcium Phosphate Dihydrate ($CaHPO_4{\cdot}2H_2O$, DCPD), Octacalcium phosphate ($Ca_8H_2(PO_4)_6{\cdot}5H_2O$, OCP), Tricalcium phosphate ($Ca_3(PO_4)_2$, β-TCP) and Hydroxyapatite ($Ca_5(PO_4)_3OH$, HAP) [1]. In hard tissues and in cases of pathological calcification, the inorganic component of the mineral salt formed is HAP. The HAP formed is generally non- stoichiometric, contains various ions (Mg^{2+}, F^-, Cl^- etc.)

*Author to whom all correspondence should be addressed.
0022-2461
DOI: 10.1007/s10853-006-2952-9

and shows poor crystallinity in comparison with the stoichiometric HAP [2]. The elucidation of the mechanism of calcium phosphates precipitation at conditions prevalent in the body fluids is still open despite the intense research conducted in the past few decades. The reason for this uncertainty is not only in the complexity of the system but also in the lack of a generally accepted methodology simulating successfully the body fluid conditions. *In vitro* studies of biological calcification may be done in an acellular simulated body fluid (SBF) with ion concentrations levels close to those corresponding to the human blood plasma chemical composition [3]. The pH control in SBF is achieved through the addition of Tris-Buffer [Tris (hydroxymethyl) Aminomethane]. Interestingly, despite the fact that the formation of crystals in solutions is very sensitive to very low levels of water soluble organic substances no attention has been paid to the effect of this compound in *in vitro* mineralization studies. Several investigators have used alternative fluid compositions defined as revised SBF [4–6] to perform biomineralisation tests in order to overcome problems associated with slow kinetics of formation of the calcium phosphate salts. The substrates tested in SBF may be classified in inorganic (e.g. various types of glasses [7, 8], gels of SiO_2, TiO_2, ZrO_2, Ta_2O_5, Nb_2O_5 [9–13], NaOH-treated Ti [14, 15] and Ta [16], silanized HAP [17]), and organic (e.g. poly (L-lactic acid) [18], arachidic acid monolayers with carboxyl groups [19] and polyethyleneterephthalate [20]). The main body of the work reported on biological calcification is focused on the preparation and characterization of biocompatible composite materials used as implants in the human body.

SBF is certainly a very useful "tool" for testing and comparing mineralization processes on various surfaces but because of its widespread use full understanding of all parameters involved in the precipitation processes is needed. Recent reports on biological calcification using SBF media, are concerned with the precipitation of calcium phosphate either at uncontrolled conditions of spontaneous precipitation in which rapid desupersaturation takes place, or at conditions in which the supply of the reactants is effected by the slow diffusion through a porous membrane [5, 6]. In these studies the heterogeneous mineralization in the SBF is achieved at very high supersaturations. In biological fluids however, the actual supersaturation may be very low due to the sequestration of the free calcium ions by the ionised macromolecules [21–23]. Detailed investigations on the thermodynamics and the kinetic stability of calcium phosphates formation in SBF solution are to the authors' knowledge very limited.

The purpose of the present work was to investigate the thermodynamics and the kinetic stability of SBF solutions maintained at physiological pH and temperature (i.e. 7.40 and 37.0°C, respectively) conditions and to measure the kinetics of formation of calcium phosphates in SBF. The use of buffer solutions was avoided and it was possible to vary supersaturation through the variation of the total calcium and phosphate concentrations within relatively narrow limits over a range that included the composition of SBF commonly found in the literature. The stability of the system was tested using the constancy of hydrogen ion activity as an indicator. In stable supersaturated SBF solutions, precipitation was initiated by the introduction of HAP seed crystals. During the course of precipitation the concentration of all species involved was kept constant through the controlled substitution of the chemicals transferred from the aqueous to the solid phases. The experimental approach presented in the present work is suggested as a high accuracy and reproducibility method for the investigation of the calcification process in SBF.

2. Experimental

2.1. *Preparation of stock solutions*

Triply distilled CO_2-free water was used for the preparation of all solutions. SBF stock solutions were prepared by dissolving $NaHCO_3$, Na_2SO_4, $MgCl_2{\cdot}6H_2O$, NaCl and KCl. The composition of SBF was in general that of the Kokubo recipe [3] except for the buffer solution and the calcium and phosphate ions. The latter components were added from the respective stock solutions to various final concentrations in the SBF resulting in different supersaturations with respect to calcium phosphates. Calcium chloride and potassium hydrogen phosphate stock solutions were prepared by dissolving the respective solids, (Merck, Puriss), and standardized as described in detail elsewhere [24]. Stock solutions were stored at 4°C until use. Sodium hydroxide and hydrochloric acid solutions were made from standard solutions (Merck, Titrisol). All solutions, prior to use were filtered through membrane filters (0.2 μm, Millipore).

2.2. *Precipitation experiments*

All experiments were done at 37.0 ± 0.1°C, in a thermostated double walled Pyrex® vessel volume totaling 0.250 dm^3, at pH 7.40. The supersaturated working solutions were prepared in the double walled vessel by mixing equal volumes (0.1 dm^3 each) of calcium and phosphate solutions, which in turn were prepared by diluting proper volumes of calcium chloride and potassium hydrogen phosphate stock solutions with the SBF stock solution. The concentrations of the ions in the working solution are shown in Table I. The working solution was checked for stability at least for 16 h. Since the precipitation of calcium phosphates from supersaturated solutions is accompanied by proton release, monitoring the solution pH was taken as the criterion for the stability of the corresponding supersaturated solutions.

A small overpressure of inert gas above the working solution was ensured with water vapor saturated pre-purified nitrogen (Linde Hellas). This was necessary in order to avoid CO_2 loss from the supersaturated SBF solution. Following the verification of the stability of the working solution from the fact that no decrease of the value of the solution pH was observed, carefully weighted (± 0.1 mg)

TABLE I Ion concentrations in the supersaturated solutions used in the present work and in human plasma [5]

Ion	Working solution/$\times 10^{-3}$ M	Human plasma/$\times 10^{-3}$ M
Na^+	142.0	142.0
K^+	5.0	5.0
Ca^{2+}	(1.5–3.3)	2.5
Mg^{2+}	1.5	1.5
HCO_3^-	4.2	27.0
Cl^-	148.0	103.0
HPO_4^{2-}	1.0	1.0
SO_4^{2-}	0.5	0.5

amounts of well characterized synthetic HAP seed crystals were introduced into the supersaturated solutions. The HAP used was prepared as follows: 1 L of 0.5 M $Ca(NO_3)_2$ and 1 L of 0.3 M $(NH_4)_2HPO_4$ were added simultaneously to 150 mL of triply distilled CO_2-free water which was kept well-stirred at 70 ± 1°C. The addition was done slowly; over a period of two hours. The pH of the solution was maintained to 10 by the addition of concentrated NH_3 and carbon dioxide was excluded by bubbling with saturated in water vapor nitrogen gas. The precipitate was washed five times with triply distilled water and refluxed at 70°C until free of NH_3. The solid was identified as stoichiometric hydroxyapatite by powder X-ray diffraction [24]. The mean particle size measured by Laser diffraction (Mastersizer S, Malvern) was found to be 8.3 μm while examination with scanning electron microscopy showed agglomerates of 50–150 nm prismatic crystallites. The specific surface area (SSA) of the seed crystals measured by nitrogen adsorption (multiple point B.E.T., Gemini, Micromeritics) was found 51.8 m^2/g.

The seeds added were well dispersed in the magnetically stirred solutions and precipitation started immediately past the introduction of HAP seed crystals. The initiation of the precipitation process resulted in proton release which, in turn, triggered the addition of titrant solutions from two mechanically coupled burettes of a modified automatic titrator (Metrohm) so as to keep the solution supersaturation constant [25–28]. The solution pH was monitored by a combination glass/saturated calomel electrode (Metrohm), calibrated before and after experiment with NBS buffer solutions [29]. The calcium chloride, potassium hydrogen phosphate and sodium hydroxide titrant solutions had the stoichiometry of the ions corresponding to hydroxyapatite: $Ca:PO_4:OH = 5:3:1$. Samples were withdrawn randomly from the solution and were filtered through membrane filters (Millipore 0.22 μm). The filtrates were analyzed for calcium and phosphate, in order to check the constancy of the solution supersaturation. The precipitated solid phases collected on the filters were examined by powder X-ray diffraction (XRD, Philips 1830/40), Fourier Transform Infrared spectroscopy (FTIR, Bruker) and Scanning Electron Microscopy equipped with an Energy Dispersive X-ray Microprobe (SEM-EDXS, JEOL ISM 5200). The particle numbers and the corresponding size distributions were measured with a laser scattering instrument (SPECTREX ILI1000). The sample of the crystals to be measured was suspended in a volume of 150 ml of saturated solution with respect to HAP to avoid dissolution. Finally, the ratio Ca/P in the precipitated solids was determined by chemical analysis for calcium and phosphate after dissolution of the precipitates in hydrochloric acid.

3. Results and discussion

The driving force for the formation of a sparingly soluble salt from a supersaturated solution is the change in Gibbs free energy, ΔG, for the transfer from a supersaturated solution to equilibrium [30]:

$$\Delta G = -\frac{R_g T}{\nu} \ln \frac{\mathrm{IP}}{K_s^0} \tag{1}$$

where IP is the ion activity product of the sparingly soluble salt (e.g. for HAP:$\mathrm{IP} = (Ca^{2+})^5(PO_4^{3-})^3(OH^-)$), K_s^0 its solubility product, ν, the number of ions in the salt, (=9 for HAP), R_g the gas constant and T the absolute temperature. The ratio IP/K_s^0 is the supersaturation ratio, Ω, and was computed with the computer code HYDRAQL [31], a free energy minimization program taking into account all equilibria in the solution, mass balance and electro neutrality conditions. The relative solution supersaturation, σ, is defined as:

$$\sigma = \Omega^{1/\nu} - 1 \tag{2}$$

The key solution variable monitored during the precipitation process was the hydrogen ion activity. This was made possible by the specialized instrumentation used and the use of buffer solutions was not necessary. A reason to avoid the use of buffer solutions (e.g. Tris-Buffer or Tris (hydroxymethyl) Aminomethane, often used in biomineralization studies) is the presence of ionized groups which may have an inhibitory role in the precipitation of the mineral phase. Preliminary experiments in our laboratory strongly supported this assumption.

The initial solution conditions and the rates of precipitation, R, obtained are summarized in Table II. It should be noted that beyond the upper limit of 3.3 mM the solutions

TABLE II Initial experimental conditions for the crystallization of calcium phosphates on synthetic HAP seed crystals in SBF solutions at conditions of constant supersaturation, at pH = 7.40 and temperature $\theta = 37°C$: Ca_t, total calcium/P_t, total phosphate = 1.67

	ΔG/kJ mol^{-1}			$R/\times 10^{-8}$
$Ca_t/\times 10^{-3}$ M)	DCPD	OCP	HAP	mol/min m^2
3.3	−0.33	−2.9	−16.5	38.6
2.5	−0.11	−2.6	−16.1	10.5
2.0	0.07	−2.3	−15.8	7.0
1.5	0.30	−1.9	−15.4	3.8

were unstable, resulting in the spontaneous formation of calcium phosphate past induction times depending on solution supersaturation. The rates of precipitation in the experiments listed in Table II, have been expressed in moles of HAP formed per unit time and unit surface area. The rates were measured from the profiles of the moles of titrants added as a function of time. These profiles correspond directly to the moles of the mineral forming. The rates were measured at very low extents of crystal growth (typically 3–5% with respect to the amount of seed added). The so calculated rates represent the kinetics of the process at a stage in which neither the solid characteristics (e.g. specific surface area, morphology) nor the solution composition have deviated from those corresponding at the start of the experiments. The extent of growth (%) is defined relatively to the amount of seed crystals used to inoculate the supersaturated solutions as follows:

$$\text{Extent of growth } \% = \frac{\text{mass deposited from titrants}}{\text{mass of seed crystals}} \times 100$$

It is interesting to note that the rates of HAP crystal growth in the SBF were comparable with the rates reported in the literature [28, 30, 31], for low ionic strength media.

As may be seen in Table II the rates of precipitation increased with increasing supersaturation with respect to HAP. The kinetics was interpreted according to the phenomenological Equation 3 [28, 31]:

$$R = k_g f(s)\sigma^n \tag{3}$$

where k_g is the precipitation rate constant, $f(s)$ a function of the active growth sites on the surface of the seed crystals introduced in the supersaturated solutions to initiate crystal growth, and the exponent n is the apparent growth order. The value of the exponent is considered to be indicative of the mechanism of the crystallization process [31–33]. The kinetics data for the crystal growth of hydroxyapatite were fitted according to Equation 3 in which the relative supersaturation was taken with respect to this phase. The curve obtained, shown in Fig. 1, suggested a parabolic dependence of the rates as a function of the solution supersaturation. This dependence, in agreement with earlier reports on the seeded growth of HAP on synthetic HAP seed crystals, suggested a surface-controlled spiral growth mechanism [34, 35]. The rate of stirring did not have any effect on the measured rates of crystallization, suggesting that the contribution of bulk diffusion to the precipitation mechanism was negligible.

In order to examine whether secondary nucleation takes place, the number and the mean size of the particles presented in the system throughout the precipitation process were measured. The measurements of the mean size were done withdrawing small aliquots which were dispersed in SBF solutions saturated with respect to HAP directly in

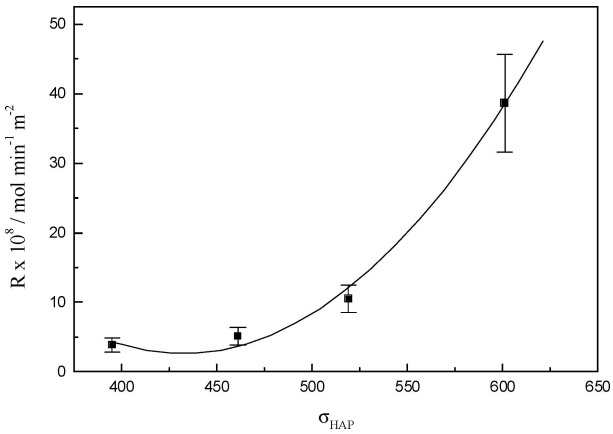

Figure 1 Rate of crystal growth of HAP seed crystals in SBF as a function of the Solution Supersaturation with respect to HAP; pH 7.40, 37°C.

the measurement cell of the laser diffraction apparatus. It was found that the number of the particles remained constant, whereas their mean size increased with time, suggesting that crystal growth took place exclusively on specific active sites on the surface of the substrate. A typical profile of the particles size evolution as a function of the extent of crystal growth is shown in Fig. 2. As may be seen, at relatively low extents of crystal growth there is almost linear dependence of the mean crystal size on the extent of crystallization. At extents of growth exceeding 100% however, although the mean crystal size was found to increase, a tendency to reach a plateau in the mean size was observed. This may be attributed to attrition of the larger HAP crystallites formed through the growth process of the seed crystals. Secondary nucleation to a small extent may also be an alternative explanation for the plateau in mean crystal size. It should be noted that the trend shown in Fig. 2 was found for all supersaturations tested. At lower supersaturations however the size increase as a function of the extent of crystal growth was

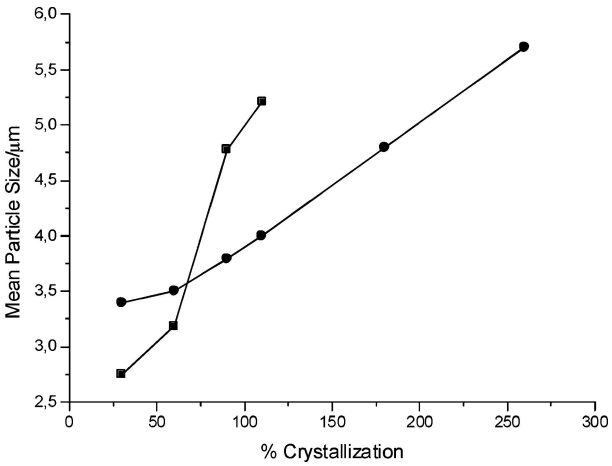

Figure 2 Dependence of the crystal size on the extent of crystallization for the growth of HAP seed crystals in SBF; (filled squares) total calcium = 1.5 mM, total phosphate = 0.89 mM; (filled circles) total Calcium = 2.5 mM, total phosphate = 1.50 mM; pH 7.40, 37°C.

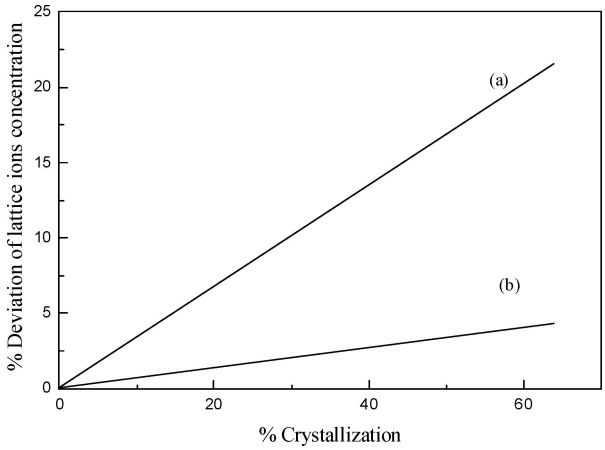

Figure 3 Deviation of the lattice ions concentrations in the SBF supersaturated solutions from their initial values as a function of the extent of crystallization: (a) Calcium ions, (b) phosphate ions; pH 7.40, 37°C. total calcium = 3.3 mM, total phosphate = 1.98 mM.

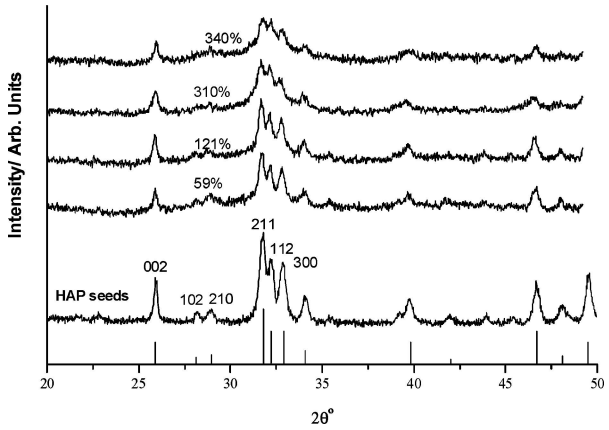

Figure 4 Powder X-ray diffraction of calcium phosphates overgrown on HAP seed crystals at different extents of growth. The lines in the bottom correspond to the reference spectral lines for HAP [35].

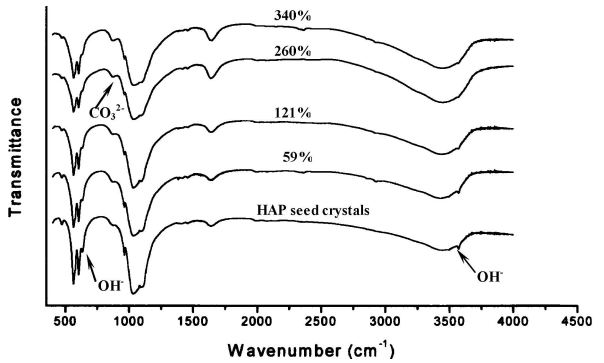

Figure 5 FTIR spectra of HAP seed crystals grown in SBF at various extents of growth, as indicated on the respective spectra.

more pronounced in comparison with that corresponding to higher supersaturations. This suggested that the higher rates of crystal growth corresponding to the higher supersaturations may affect the shape of the crystallites formed.

One of the important advantages of the constant composition experimental approach is the direct information on the stoichiometry of the precipitating phase. Since the titrant solutions contain the lattice ions of the crystallizing phase with the corresponding stoichiometry, it is expected that their concentration in solution does not vary significantly from that of the initial supersaturated solution. Should a solid form with stoichiometry other than the anticipated, the concentration of the lattice ions in the working solution would deviate from their initial values. Thus, calcium in solution is not expected to remain constant if a transient phase (e.g. OCP), with a stoichiometry different than that of the inoculating seed crystals forms. In the SBF supersaturated solutions the ion concentrations deviated from the initial values with increasing extent of crystallization, as may be seen in Fig. 3.

Considering that the titrant solutions in the experiment corresponding to Fig. 3, were prepared with the stoichiometry of HAP, the observed concentration changes implied that a calcium phosphate phase with stoichiometry different from that of HAP formed on the HAP seed crystals. Alternatively, the deviation from the stoichiometry of HAP may be due to the presence of foreign ions incorporated into the apatite lattice during the crystal growth stage. Since the phosphate concentration in solution did not change practically, this should be interpreted as a confirmation that the solid precipitated contained the phosphate anticipated but less of the calcium. The stoichiometry deviations may be attributed to the replacement of Ca^{2+} ion with a different cation like Mg^{2+} or Na^+. Both ions are commonly found in biological apatites [28].

The powder XRD spectra of the precipitated solids shown in Fig. 4 showed that the (211), (112) and (300) reflections were less well separated with increasing extent of crystal growth. In seeded growth experiments of stoichiometric HAP on HAP seed crystals, the crystallinity of the solid increased significantly with increasing extent of crystal growth [22]. The decreasing crystallinity of the solids formed with increasing extent of crystal growth may suggest the transformation of transient phases to apatitic phase (non-stoichiometric HAP) [28].

The suggestion of the formation and transformation of transient calcium phosphate phases is corroborated by the fact that the molar ratio Ca/P in the precipitated solids was reduced with increasing extent of crystal growth, as shown in Table III.

TABLE III Molar ratio Ca/P of the precipitated solids obtained at different crystallization percentages in SBF; $Ca_t = 1.5 \times 10^{-3}$ M, 37°C, pH 7.40

Ca/P	(%) Extent of crystal growth
1.67	0
1.52	82
1.44	121
1.17	200

The FT-IR spectra of the precipitated solids are shown in Fig. 5. At higher extents of growth with respect to the seed crystals, the bands at 875 cm^{-1} corresponding to the carbonate vibration mode were more pronounced, suggesting respective increase in the carbonate content of the mineral formed. It is possible that the carbonate replace phosphate ions during the crystal growth process [37, 38]. Reports on bone maturation have concluded that carbonate ions are initially located on the surface of the mineral displacing acid phosphate ions (HPO_4^{2-}) [39]. The bands corresponding to the OH^- ions (3570 and 634 cm^{-1}) decreased as may be seen in the spectra of the precipitated solids presented in Fig. 5.

The morphological examination of the obtained precipitates corroborated further the spectroscopic findings. In Fig. 6a the morphology of the seed crystals is shown. The crystals used to seed the supersaturated SBF solutions had a prismatic habit and their size was approximately 100 nm. Upon crystallization in the SBF morphological changes were visible as may be seen in Fig. 6b and c in which plate-like formations were visible with sizes of approximately 1 μm. These formations may be due either to the formation of transient phases or to morphological changes due to carbonate incorporation. At the same time the seed crystals increased in size with increasing extent of crystal growth at constant supersaturation.

The microanalysis of the precipitates revealed the presence of Mg as may be seen in the spectra presented in

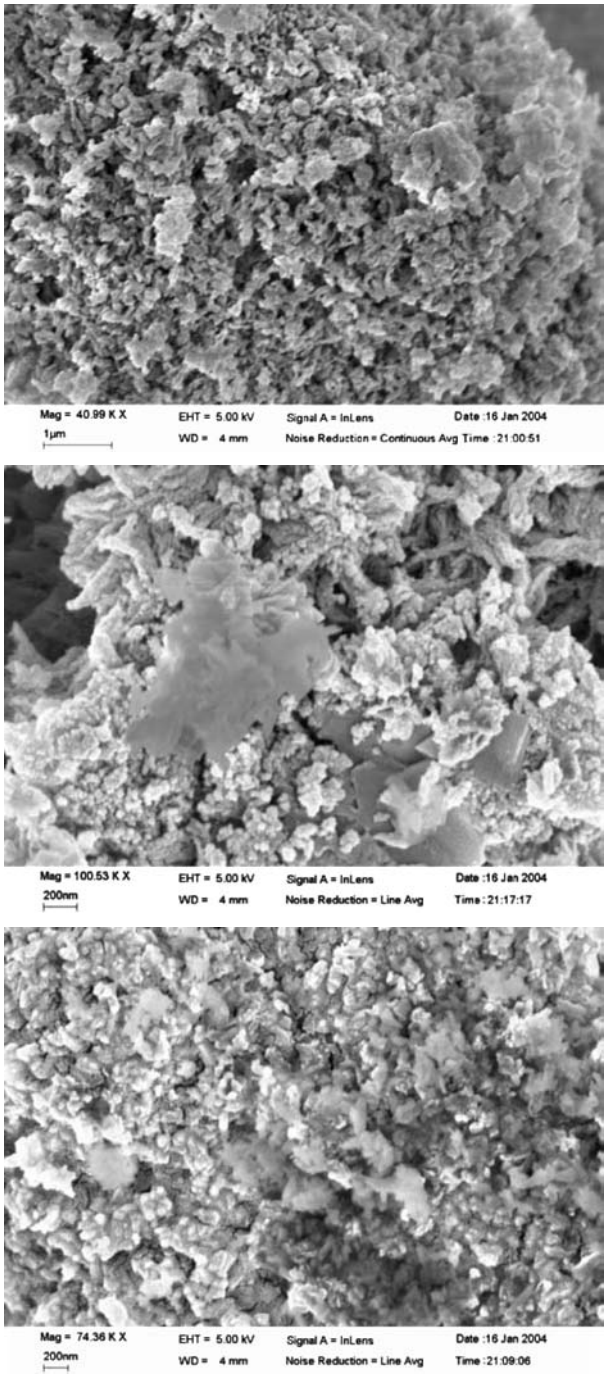

Figure 6 SEM of HAP crystals: (a): Seed crystals (bar = 1 μm); (b) grown in SBF at 37°C, pH 7.40; 118% of growth with respect to seed crystals: $Ca_t = 1.5 \times 10^{-3}$ M (bar 200 nm). (b) grown in SBF at 37°C, pH 7.40; 132% of growth with respect to seed crystals: $Ca_t = 2.0 \times 10^{-3}$ M (bar 200 nm).

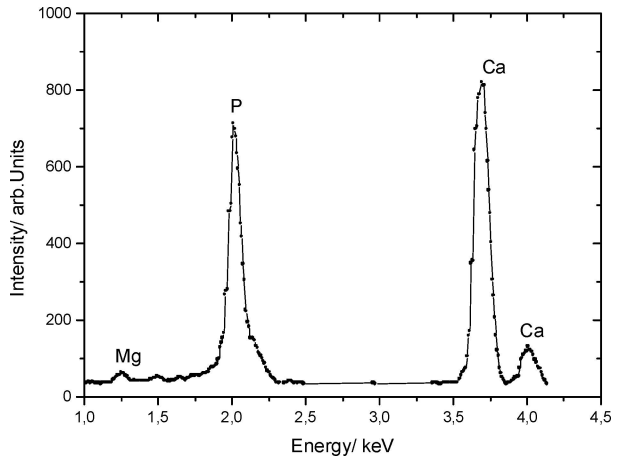

Figure 7 EDXS microanalysis of the precipitate formed through the crystallization of HAP seed crystals in SBF at 37°C, pH 7.40; 120% of growth with respect to seed crystals.

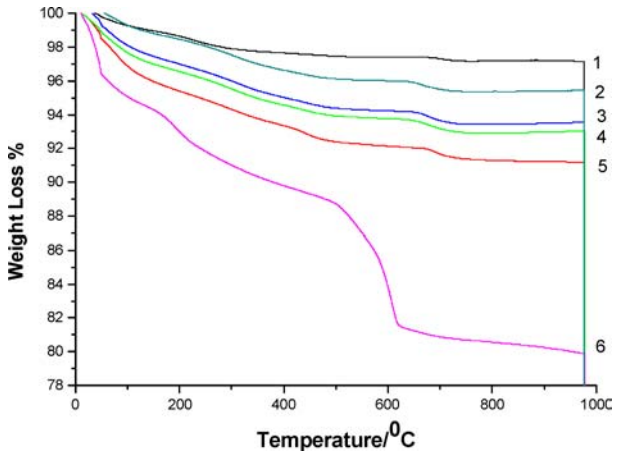

Figure 8 Thermo gravimetric analysis of solid samples in air atmosphere; 1: Seed crystals prepared synthetically; 2: 82% with respect to seed crystals; 3: 121% with respect to seed crystals; 4: 200% with respect to seed crystals; 5: 340% with respect to seed crystals; 6: Carbonated apatite.

Fig. 7. This finding is in agreement with reports that the growth of HAP in SBF solutions results in the incorporation of sodium and magnesium [4]. It may thus be concluded that the solid precipitated on HAP seed crystals in SBF solutions consists of carbonate and magnesium substituted HAP [40].

The weight loss measurement as a function of temperature for the calcium phosphate precipitated in SBF media supported further the incorporation of the carbonate ions. The results of thermo gravimetric analysis of the precipitates may be seen in Fig. 8. Comparison of the curves 1–5 of Fig. 8 with curve 6 shows that the inflection observed in the range 635–650°C corresponds mainly to the loss of carbonate [41, 42] amounting to approximately 1%.

4. Conclusions

In the present work, the crystallization of HAP in SBF solutions without the use of potentially interfering buffer solutions like the Tris-buffer, was investigated using a pH-stat-constant supersaturation technique. The upper limit of the stability of the SBF solutions was found to be at supersaturations corresponding to a total calcium concentration of 3.3 mM and total calcium to total phosphate molar ratio of 1.67. In the stable region of SBF solutions the growth of HAP seed crystals showed second order dependence on the supersaturation. This dependence suggested a surface-controlled mechanism. Crystal growth took place exclusively on specific active sites on the surface of the seeds. The incorporation of foreign ions into the crystalline phase and/or the formation of transient calcium phosphate phases caused deviations from the constancy of the solution composition. Chemical analysis of the precipitates showed that carbonate and magnesium ions from the SBF solution were incorporated into the HAP crystal lattice. On the basis of the morphology of the precipitated solids and the thermodynamic calculations for the relatively high supersaturation in the SBF solutions tested, it may also be suggested that the formation of transient phases like OCP less stable than HAP is possible. The HAP crystals showed prismatic habit with crystallites in the size range of a few decades of nm. The formation of precursors with plate-like habit may be attributed to kinetic stabilization due to the presence of carbonate ions in the supersaturated SBF solutions.

Acknowledgements

The authors wish to acknowledge with appreciation financial support by the ministry of Education through the EPEAEK II programme.

References

1. G. H. NANCOLLAS, in "Biomineralization, Chemical and Biochemical Perspectives," edited by S. Mann, J. Webb and R.J.P. Williams (VCH Publ. Weinheim 1989) p. 157.
2. P. G. KOUTSOUKOS, in "Calcium Phosphates in Biological and Industrial Systems," edited by Z. Amjad (Kluwer Acad. Publ., Boston, 1988) p. 145.
3. T. KOKUBO, H. KUSHITANI, S. SAKKA, T. KITSUGI and T. YAMAMURO, *J Biomed Mater Res.* **24** (1990) 721.
4. S. V. DOROZHKIN, E. I. DOROZHKINA and M. EPPLE, *J. Appl. Biomate. & Biomecha.* **1** (2003) 200.
5. S. V. DOROZHKIN and E. I. DOROZHKINA, *Colloids and Surfaces A: Physicochem. Eng. Aspects* **215** (2003) 191.
6. *Idem., ibid.* **223** (2003) 231.
7. H.-M. KIM, T. MIYAZAKI, T. KOKUBO and T. NAKAMURA, in "Bioceramics 13," edited by S. Giannini and A. Moroni (Trans. Tech Publications 2001) Vol. 47 p. 192.
8. A. BIGI, E. BOANINI, S. PANZAVOLTA and N. ROVERI, *Biomacromolecules* **1** (2000) 752.
9. T. KOKUBO, H.-M. KIM, M. KAWASHITA and T. NAKAMURA, *Z. Kardiol.* **90** (2001) III86.
10. A. RAMILA and M. VALLET-REGI, *Biomaterials* **22** (2001) 2301.
11. M. UCHIDA, H.-M. KIM, T. KOKUBO, F. MIYAJI and T. NAKAMURA, *J. Am. Ceram. Soc.* **84** (2001) 2041.
12. E. RIVERA-MUNOZ, W. BROSTOW, R. RODRIGUEZ and V. M. CASTANO, *Mat. Res. Innovation* **4** (2001) 222.
13. J. M. GOMEZ-VEGA, A. HOZUMI, H. SUGIMURA and O. TAKAI, *Adv. Mater.* **13** (2001) 822.
14. H. TAKADAMA, H.-M. KIM, T. KOKUBO and T. NAKAMURA, *J. Biomed. Mat. Res.* **57** (2001) 441.
15. S. FUJIBAYASHI, T. NAKAMURA, S. NISHIGUCHI, J. TAMURA, M. UCHIDA, H.-M. KIM and T. KOKUBO, *ibid.* **56** (2001) 562.
16. T. MIYAZAKI, H.-M. KIM, T. KOKUBO, F. MIYAJI, H. KATO and T. NAKAMURA, *J. Mater. Sci: Mater. Med.* **12** (2001) 683.
17. C. SANTOS, Z. B. LUKLINSKA, R. L. CLARKE and K. W. M. DAVY, *ibid.* **12** (2001) 565.
18. X. Y. YUAN, A. F. T. MAK and J. L. LI, *J. Biomed. Mat. Res.* **57** (2001) 140.
19. K. SATO, T. KOGURE, Y. KUMAGAI and J. TANAKA, *J. Coloidl Interf. Sci.* **240** (2001) 133.
20. H.-M. KIM, K. KISHIMOTO, F. MIYAJI, T. KOKUBO, T. YAO, Y. SUETSUGU, J. TANAKA and T. NAKAMURA, *J. Mater. Sci. Mater. Med.* **11** (2000) 421.
21. B. TOMAZIC and G. H. NANCOLLAS, *J. Coll. Interf. Sci.* **50** (1975) 451.
22. B. TOMAZIC, M.B. TOMSON and G.H. NANCOLLAS, *Calcified Tissue Research* **19** (1976) 263.
23. A. L. BOSKEY and A. S. POSNER, *J. Phys. Chem.* **80** (1976) 40.
24. J. C. ELLIOTT, Structure and Chemistry of the Apatites and Other Calcium Orthophosphates (Amsterdam: Elsevier, 1994).
25. P. G. KOUTSOUKOS, Z. AMJAD, M. B. TOMSON and G. H. NANCOLLAS, *J. Am. Chem. Soc.* **102** (1980) 1553.
26. M. B. TOMSON and G. H. NANCOLLAS, *Science* **200** (1978) 1059.
27. Z. AMJAD, P. G. KOUTSOUKOS and G. H. NANCOLLAS, *J. Coll. Interf. Sci.* **101** (1984) 250.
28. J. C. HEUGHEBAERT, S. ZAWACKI and G. H. NANCOLLAS, *ibid.* **135** (1990) 20.
29. R. G. BATESM, pH Determination (J. Wiley, New York, 1967)
30. P. G. KOUTSOUKOS, in Calcium Phosphates in Biological and Industrial Systems, edited by Z. Amjad (Kluwer Acad. Publ., Boston, 1998) p. 41.
31. G. PAPELIS, K. F. HAYES and J. O. LECKIE, HYDRAQL, A Program for the Computation of Chemical Equilibrium Composition of Aqueous Batch Systems Including Surface Compexation Modelling of Ion Association at the Oxide/Solution Interface. Technical Report No. 306 (Stanford University, Stanford, CA, 1988).
32. M. DALPI, E. KARAYIANNI and P. G. KOUTSOUKOS, *J. Chem. Soc. Faraday Trans.* **89** (1993) 965.

33. J. KAPOLOS and P. G. KOUTSOUKOS, *Langmuir* **15** (1999) 6557.
34. N. SPANOS and P. G. KOUTSOUKOS, *J. Mater. Sci.* **36** (2001) 573.
35. G. H. NANCOLLAS and M. S. MOHAN, *Archs. Oral Biol.* **15** (1970) 731.
36. P. G. KOUTSOUKOS and G. H. NANCOLLAS, *J. Crys. Grow.* **53** (1981) 10.
37. K. SANGWAL, in "Elementary Crystal Growth" edited by K. Sangwal (Saan Publishers, Lublin, Poland, 1994) p. 83.
38. International Center for Diffraction Data, JCPDS, File Card No 9-0430 (1996).
39. D. G. A. NELSON and J. D. B. FEATHERSTONE, *Calcif. Tissue Int.* **34** (1982) S69.
40. J. BARRALET, S. BEST and W. BONEFIELD, *J. Biomed. Mater. Res.* **41** (1998) 79.
41. X. GUOFENG, A. A. ILHAN and J. T. GROVES, *J. Amer. Chem. Soc.* **123** (2001) 2196.
42. D. TADIC, F. PETERS and M. EPPLE, *Biomaterials* **23** (2002) 2553.

Received 25 October 2004
and accepted 13 June 2005